Electronic Supplementary Material (ESI) for Journal of Materials Chemistry C.

Supporting Information for

Highly efficient and stable planar perovskite solar cells enabled by $K_3[Fe(CN)_6]$-doped spiro-OMeTAD

Weihai Sun, Mingjing Zhang, Shibo Wang, Fengxian Cao, Jinjun Zou, Yitian Du, Zhang Lan, Jihuai Wu*

Engineering Research Center of Environment-Friendly Functional Materials, Ministry of Education;

Fujian Engineering Research Center of Green Functional Materials;

Institute of Materials Physical Chemistry, Huaqiao University, Xiamen 361021, China

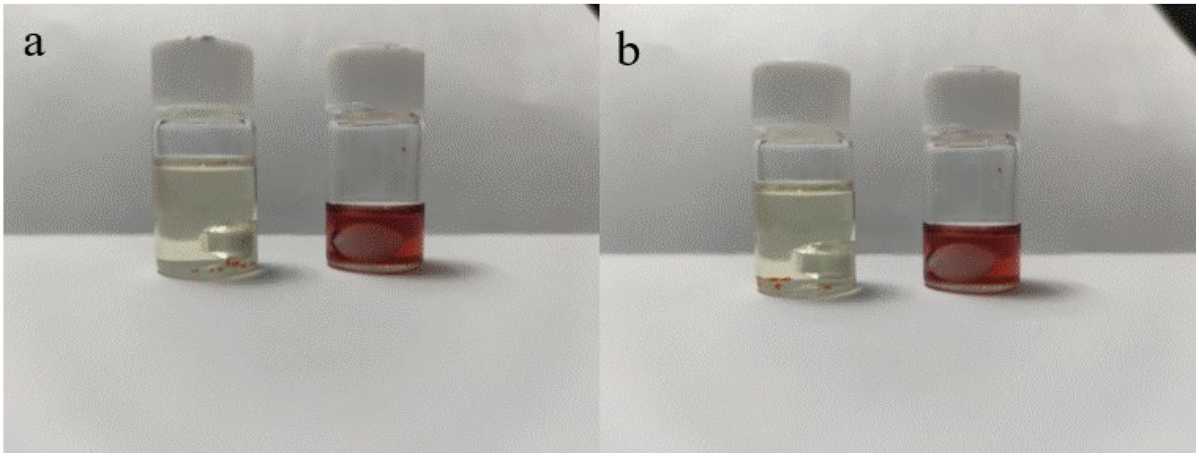

Fig. S1 (a) Photograph of $K_3[Fe(CN)_4]$-doped spiro-OMeTAD solutions with acetonitrile (left) and Li-TFSI+tBP (right) .(b) Photograph of $K_3[Fe(CN)_4]$-doped spiro-OMeTAD solutions with tBP (left) and Li-TFSI+tBP (right).

E-mail: jhwu@hqu.edu.cn (J. Wu.)

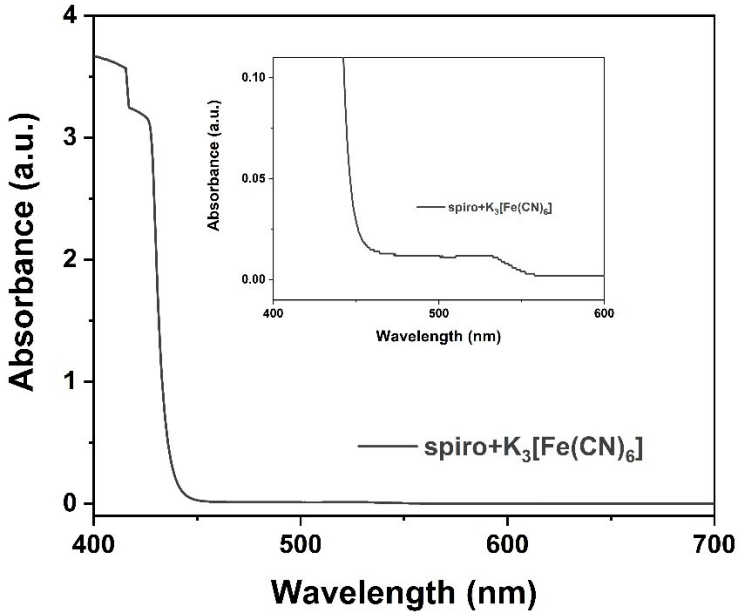

Fig. S2 UV-Vis absorption spectra of spiro-OMeTAD solution with only $K_3[Fe(CN)_4]$.

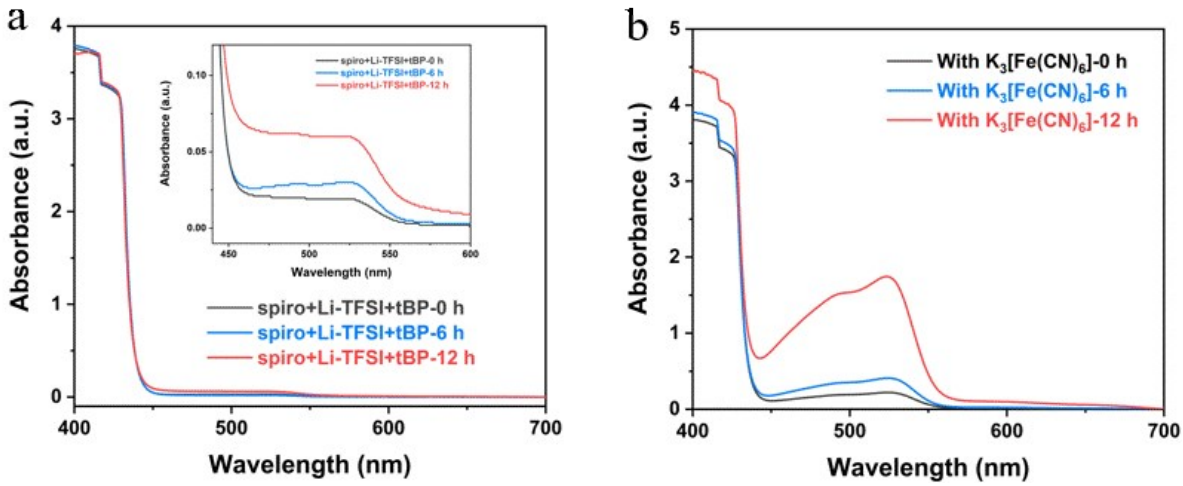

Fig. S3 UV-Vis absorption spectra of spiro-OMeTAD solution without (a) and with $K_3[Fe(CN)_4]$ (b) in the presence of Li-TFSI and tBP at different oxidation times of 0, 6 and 12 h.

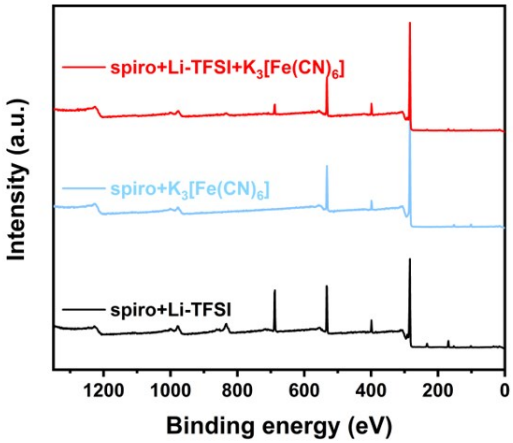

Fig. S4 The survey spectra for the HTM doped with various additives.

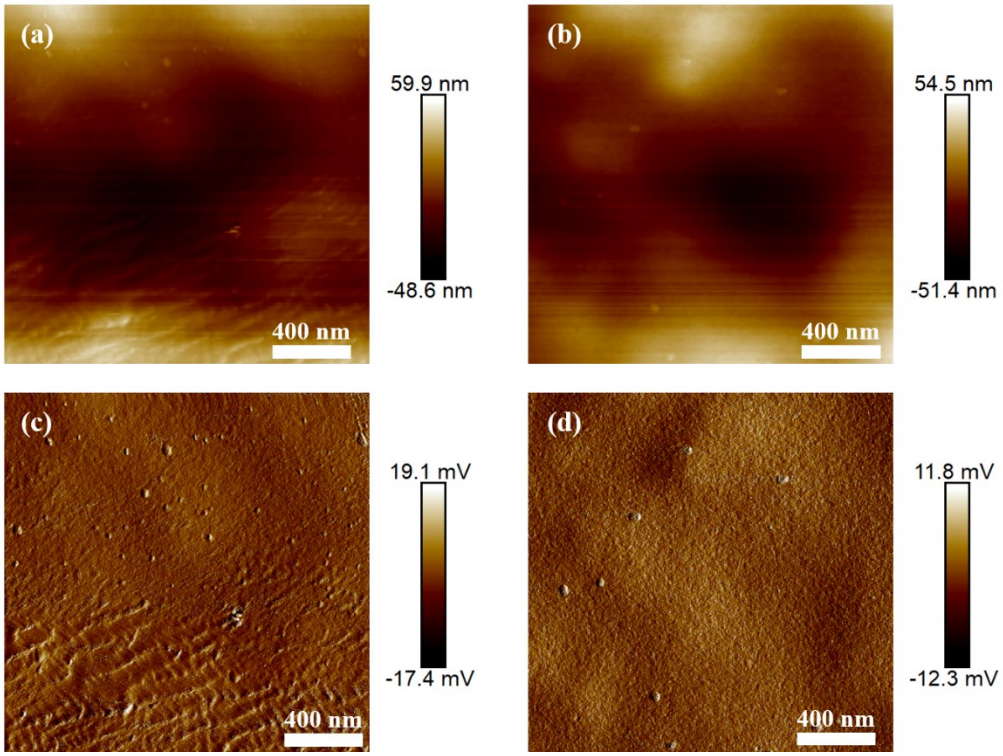

Fig. S5 Tapping mode and intelligent mode AFM topography images of pristine (a and c) and $K_3[Fe(CN)_4]$-doped spiro-OMeTAD (b and d).

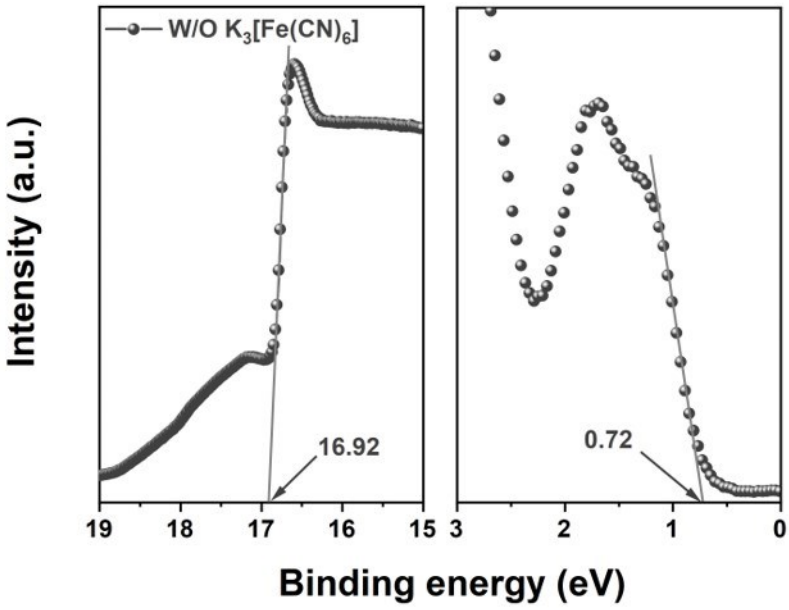

Fig. S6 The UPS spectra for spiro-OMeTAD without $K_3[Fe(CN)_4]$ (left: E_{cutoff} region; right: E_{onset} region).

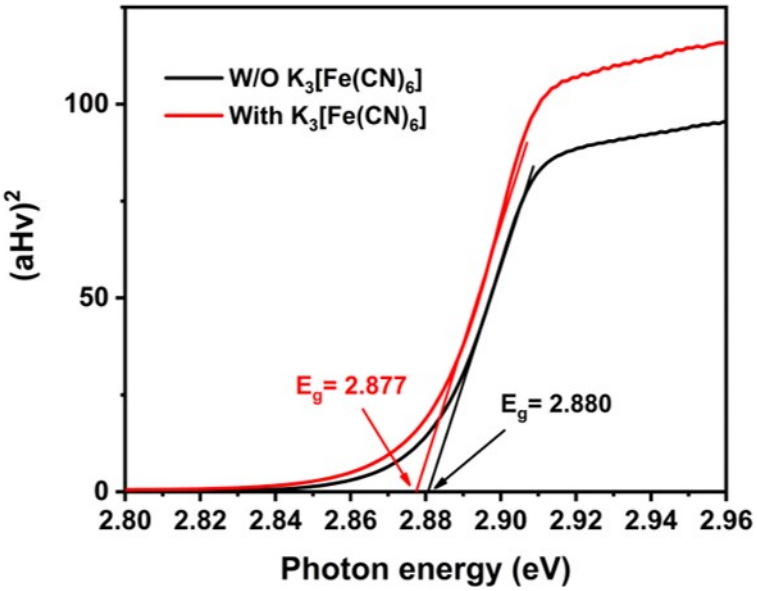

Fig. S7 Tauc plots of the spiro-OMeTAD films with and without $K_3[Fe(CN)_4]$.

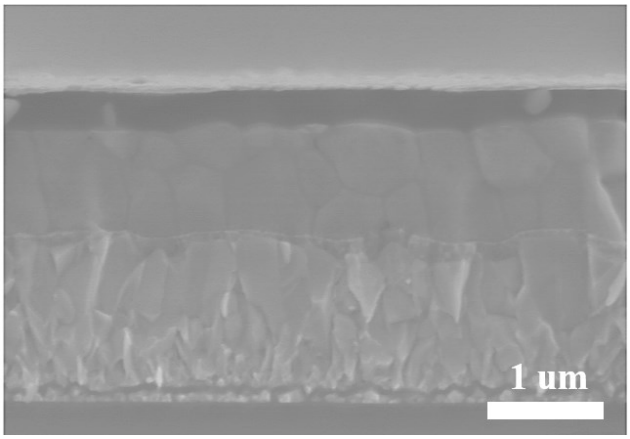

Fig. S8 Cross-view SEM image of the undoped PSC device.

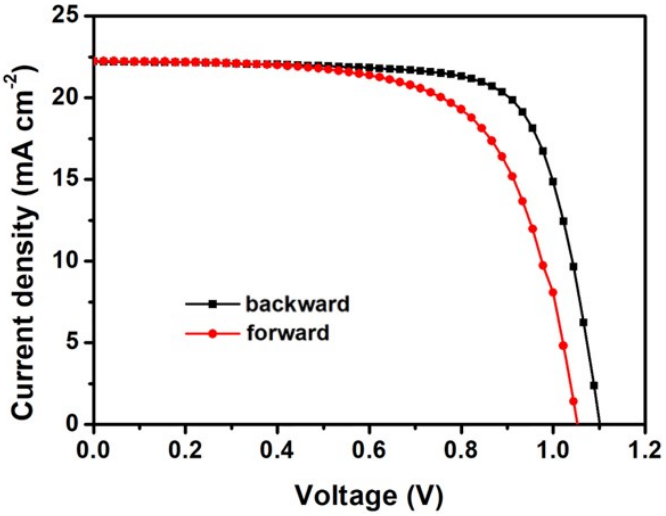

Fig. S9 The *J-V* curves of pristine PSCs measured with both forward and backward scans.

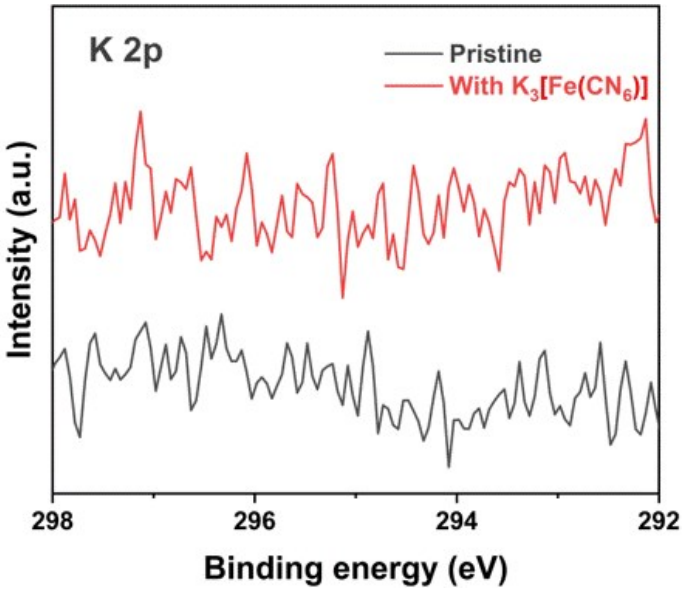

Fig. S10 High resolution K 2p XPS spectra of the perovskite films which are firstly covered with $K_3[Fe(CN)_4]$-doped and pristine HTL and then washed by chlorobenzene.

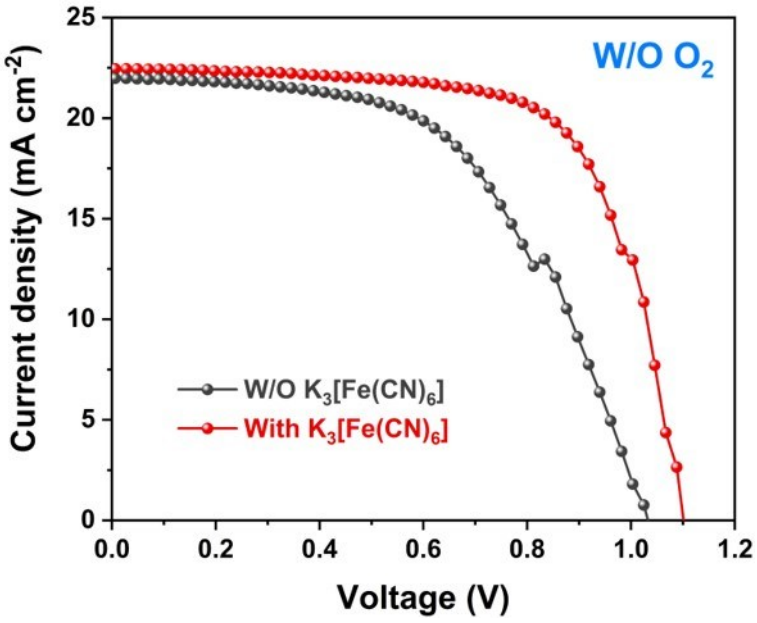

Fig. S11 The *J-V* curves of pristine and $K_3[Fe(CN)_4]$-modified PSCs without the overnight pre-oxidation.

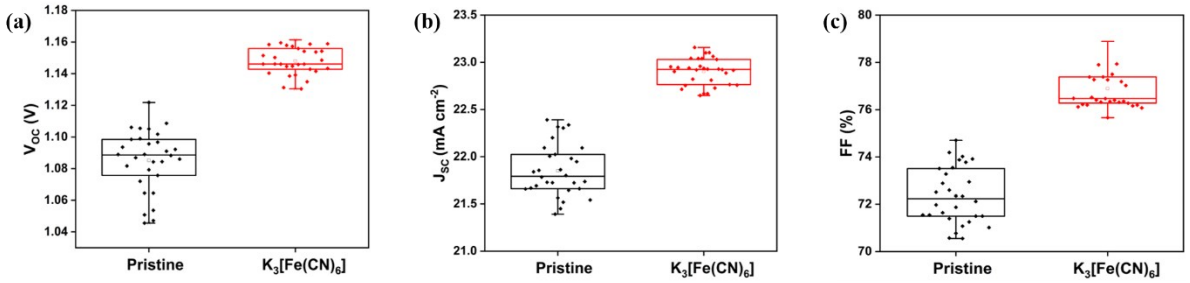

Fig. S12 The statistical data of V_{oc}, J_{sc} and FF based on 30 independent pristine and $K_3[Fe(CN)_4]$-doped devices.

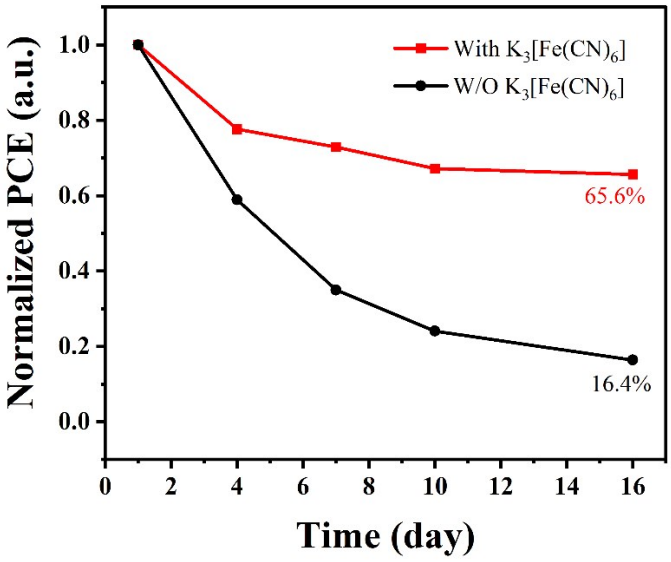

Fig. S13 The long-term stability of solar cells with and without $K_3[Fe(CN)_4]$ for 16 days.

Table S1. The conductivity values of the HTLs doped with different dopants.

HTL with different dopants	Conductivity (S cm^{-1})
None	6.84×10^{-4}
$K_3[Fe(CN)_4]$	6.99×10^{-4}
Li-TFSI+tBP	7.66×10^{-4}
$K_3[Fe(CN)_4]$+ Li-TFSI+tBP	1.09×10^{-3}

Table S2. Photovoltaic data of PSCs based on HTLs doping with different concentrations of $K_3[Fe(CN)_4]$

$K_3[Fe(CN)_4]$ concentration (mg mL^{-1})	V_{OC}(V)	J_{SC} (mA cm^{-2})	FF	PCE (%)
0	1.10	22.22	0.74	18.09
0.6	1.13	22.89	0.75	19.40

0.8	1.16	23.03	0.78	20.83
1.0	1.16	22.92	0.75	19.94

Table S3. Photovoltaic data of pristine and $K_3[Fe(CN)_4]$-modified devices with different scan directions.

Device	Scan direction	V_{OC} (V)	J_{SC} (mA cm^{-2})	FF	PCE (%)	HI
Pristine	Backward	1.10	22.22	0.74	18.09	0.157
	Forward	1.04	22.23	0.66	15.25	
$K_3[Fe(CN)_4]$-modified	Backward	1.15	23.10	0.76	20.19	0.072
	Forward	1.10	22.98	0.74	18.70	

Table S4. Photovoltaic parameters of pristine and $K_3[Fe(CN)_4]$-modified PSCs without the overnight pre-oxidation

devices	V_{OC}(V)	J_{SC} (mA cm^{-2})	FF	PCE (%)
Pristine	1.03	21.99	0.54	12.23
$K_3[Fe(CN)_4]$	1.10	22.46	0.68	16.80

Table S5. TRPL data of FTO/perovskite and FTO/perovskite/spiro-OMeTAD with different dopants.

samples	τ_{ave} (ns)	A_1 (%)	τ_1 (ns)	A_2 (%)	τ_2 (ns)
Perovskite	52.06	22.28	10.89	77.72	63.86

Perovskite/spiro-OMeTAD	17.45	47.09	5.822	52.91	27.80
Perovskite/spiro-OMeTAD with $K_3[Fe(CN)_4]$	8.21	53.42	2.70	46.58	14.53